

Supporting Information

CoOx-caged Metal-organic Frameworks for Sonocatalyzing CO₂ to CO for
Ultrasound-assisted Chemodynamic-Gas Cancer Therapy

Tian Zhang^{1, □}, *Qiang Zheng*^{2, □}, *Jie Huang*^{4*}, *Xiang Li*^{1,3*}

¹ State Key Laboratory of Silicon and Advanced Semiconductor Materials, School of Materials Science and Engineering, Zhejiang University, Hangzhou, Zhejiang 310058, P. R. China

² Key Laboratory of Endoscopic Technique Research of Zhejiang Province, Sir Run Run Shaw Hospital, Zhejiang University, Hangzhou 215123, P. R. China

³ ZJU-Hangzhou Global Scientific and Technological Innovation Center, Zhejiang University, Hangzhou, 311200, P.R. China.

⁴ Department of Mechanical Engineering, University College London, London WC1E 7JE, UK

* Corresponding Author: jie.huang@ucl.ac.uk; xiang.li@zju.edu.cn (XL)

□ Authors with equal contribution

2.1 Chemicals and Agents

Terephthalic acid was obtained from Xushuo Biotechnology Co., Ltd. Ammonium fluoride (NH_4F), Hydrofluoric acid (HF, 46wt%), N, N-Dimethylformamide (DMF) and hexane were purchased from Sinopharm Chemical Reagent Co., Ltd. Chromium (III) nitrate nonahydrate ($\text{Cr}(\text{NO}_3)_3 \cdot 9\text{H}_2\text{O}$) and Cobalt nitrate hexahydrate ($\text{Co}(\text{NO}_3)_2 \cdot 6\text{H}_2\text{O}$) were purchased from Aladdin Co., Ltd. Hemoglobin was purchased from Macklin. RPMI 1640 medium and DMEM high glucose culture medium with 1% penicillin-streptomycin were purchased from Senrui Biotechnology Co., Ltd. Fetal bovine serum (FBS) was purchased from Dalian Meilun Biotechnology Co., Ltd. CAY10733 was purchased from Dawen Biotechnology Co., Ltd. 2',7'-dichlorodihydrofluorescein diacetate (DCFH-DA, $\geq 97\%$) were purchased from Sigma-Aldrich. Mitochondrial membrane potential assay kit with JC-1 was obtained from Beyotime Biotechnology. All of the agents in the experiments were analytic grade or higher and used without further purification.

2.2 Synthesis of MIL-101(Cr)@CoOx

2.2.1 Synthesis of MIL-101(Cr) MOF

The MIL-101(Cr) nanoparticles was synthesized by a modified hydrothermal method reported previously^[1]. Briefly, terephthalic acid (1.6 g), $\text{Cr}(\text{NO}_3)_3 \cdot 9\text{H}_2\text{O}$ (4.0 g) and HF solution (175 μL) were dissolved in deionized water (70 mL). The solution was transferred into Teflon-lined stainless-steel autoclave and heated at 220°C for 8 h. To remove the residual terephthalic acid inside the MIL-101(Cr) pores, the as-prepared MIL-101(Cr) suspension was washed with DMF at the room temperature (x 3), then purified using ethanol at 100°C for 24 h and NH_4F solution (37.5 mmol, 30 mL) at 70°C for

10h. The green product was centrifuged and washed with hot water (x 3). Finally, the products were dried under vacuum at 60°C overnight.

2.2.2 Synthesis of MIL-101(Cr) and CoOx composites MIL-101(Cr)@CoOx

The as-made MIL-101(Cr) powder (100 mg) was dispersed in hexane (20 mL), then mixed with $\text{Co}(\text{NO}_3)_2 \cdot 6\text{H}_2\text{O}$ (400 μL , 0.4 M) and stirred at room temperature for 2 h. The mixture was washed with hexane (x 3). The obtained product was dried under vacuum at 60°C overnight.

The collected powder was calcined in 5% H_2/N_2 atmosphere at 250°C for 3 h and 150°C for 2 h, sequentially. The heating/cooling rate was 5°C min^{-1} . As a test control, CoOx nanoparticles were prepared from the same $\text{Co}(\text{NO}_3)_2 \cdot 6\text{H}_2\text{O}$ powder and using the same protocol described above. The incorporation of Co content in MIL-101(Cr)@CoOx was measured using an inductively coupled plasma optical emission spectrometer (ICP-OES) (ICP6000, Thermo Fisher, UK).

2.3 Characterizations of MIL-101(Cr)@CoOx

The scanning electron microscopy (SEM) and transmission electron microscopy (TEM) observation were performed on Phenom LE field-emission SEM and JEPL JEM-2010HR TEM (200 kV), respectively. The elemental composition was characterized using energy-dispersive X-ray spectroscopy (EDS), FEI Tecnai F20. Rigaku D/Max-2550pc powder diffractometer was used to collect XRD patterns, scanning 2θ from 5° to 80°. The valence state and valence band (VB) potential of MIL-101(Cr)@CoOx were measured by X-ray photoelectron spectroscopy (XPS, Thermo Scientific K-Alpha). The ζ -potential analysis was conducted using Zetasizer Nano-ZS (Malvern, UK).

2.4 CO₂ gas adsorption measurements

The gas adsorption capacity of MIL-101(Cr)@CoOx was measured using a Micromeritics ASAP 2020 surface area analyzer, and compared with those of CoOx and MIL-101(Cr) test control materials. Before the measurement of CO₂ gas adsorption, the test materials were pre-activated at 50°C under vacuum (3 μmmHg) for 12 h in gas adsorption apparatus. The measurements were preceded at 77 K using a liquid nitrogen bath and at 196 K using a drikold bath. Then the adsorption isotherms for CO₂ of the three samples were measured at 37°C, using a water bath.

2.5 Conversion of CO₂ to CO assisted by ultrasound irradiation

CO binds to hemoglobin (Hb) competitively, forming carboxyhemoglobin (HbCO) complex, and the binding rate is stronger and quicker than that of oxygen. A hemoglobin (Hb) binding assay was used to measure the generation of CO under ultrasound stimulation.

Briefly, bovine hemoglobin (4.2 μM) was fully dissolved into PBS (1×, pH = 7.4) solution. The hemoglobin solution was degassed firstly after bubbling with nitrogen gas for 30 min, and sodium hydrosulfite (10 mg) was added thereafter to prepare the deoxygenated hemoglobin. MIL-101(Cr)@CoOx (with a final concentration of 60 μg mL⁻¹) was then mixed with the deoxygenated hemoglobin. The solution was irradiated by an ultrasound (WED-100, Shenzhen Well.d MEDICAL Electronics Co., Ltd.) at 1 MHz with intensity of 0.5 W cm⁻² for 5 min. The level of HbCO was recorded by a UV-Vis spectrophotometer (Shimadzu UV-2600) from 380 nm to 600 nm.

The CO concentration was quantified according to the Beer-Lambert law. As the HbCO and Hb adsorption bands observed at 420 nm and 430 nm, respectively, the HbCO level were calculated

according to the following function:

$$C_{CO} = \frac{528.6 \times I_{420 \text{ nm}} - 304 \times I_{430 \text{ nm}}}{216.5 \times I_{420 \text{ nm}} + 442.4 \times I_{430 \text{ nm}}} C_{Hb}$$

wherein, C_{CO} and C_{Hb} are the concentration of generated CO and the initial concentration of Hb, respectively; $I_{420 \text{ nm}}$ and $I_{430 \text{ nm}}$ are the absorbance values at 420 nm and 430 nm, respectively^[2].

For the test controls, the standard HbCO and HbO₂ complex references, prepared by bubbling of CO and O₂ to the deoxygenated hemoglobin solutions, were measured using the UV-Vis spectrophotometer and photographed for a record and comparison.

2.6 Chemodynamic activity of MIL-101(Cr)@CoOx

The generation of ROS from MIL-101(Cr)@CoOx in Fenton-like reaction was evaluated using 3,3',5,5'-Tetramethylbenzidine (TMB) oxidation assay. Briefly, TMB (0.8 mM, ethanol solution) and H₂O₂ (1 mM) was added into MIL-101(Cr)@CoOx (100 μg mL⁻¹) solution. After reacting for 3 min, the absorbance from 400 nm to 800 nm was measured using the UV-Vis spectrophotometer. The absorbances of TMB, TMB/H₂O₂ and TMB/MIL-101(Cr)@CoOx were also recorded for comparisons. To further quantify the chemodynamic activity of MIL-101(Cr)@CoOx, the measurement at 653 nm was carried out at variable concentrations of H₂O₂ (from 0.5 mM to 10 mM) with a fixed concentration of TMB (0.8 mM) and MIL-101(Cr)@CoOx (100 μg mL⁻¹).

The production of OH radicals during the Fenton-like reaction was also measured using 5,5-Dimethyl-1-pyrroline N-oxide (DMPO) assay. Briefly, 160 μl MIL-101(Cr)@CoOx (100 μg mL⁻¹)/H₂O₂ (1 mM) mixture was added to DMPO (40 μl), and the resultant DMPO-OH spin adducts were detected by electron spin resonance (ESR) measurement on a Bruker A300 X-band EPR spectrometer.

To evaluate the effects of ultrasound on Fenton activity of MIL-101(Cr)@CoOx, the MIL-101(Cr)@CoOx (100 $\mu\text{g mL}^{-1}$) solution was subjected to ultrasound (1.0 MHz, 2.0 W cm^{-2}) irradiation for 5 min, then the generation of ROS was measured using the TMB assay every minute up to 5 minutes.

The potential release of Co ions from MIL-101(Cr)@CoOx after the ultrasound treatment was also measured using an inductively coupled plasma optical emission spectrometer (ICP-OES) (ICP6000, Thermo Fisher, UK)

2.7 Cell culture

AML12 mouse hepatocytes and Mouse 4T1 breast cancer cells used for the *in vivo* experiments, were obtained from Sir Run Shaw Hospital, Zhejiang University (Hangzhou, China). 4T1 breast cells and AML12 cells were cultured in RPMI 1640/10% FBS medium and DMEM/10% FBS medium, respectively, at 37°C in a humidified incubator of 5% CO₂.

2.7.1 Methyl thiazolyl tetrazolium (MTT) assay

The *in vitro* cell biocompatibility of MIL-101@CoOx was evaluated using the AML12 mouse hepatocytes cell model. In brief, AML12 cells were seeded into 96-well plates ($\sim 10^4$ cells per well) and grown for 12-16 h. Then different concentrations of MIL-101@CoOx (from 0 to 100 $\mu\text{g mL}^{-1}$) was added to the culture. After 24 h incubation, the cell viability was assessed using MTT assay according to the standard protocol^[3].

The *in vitro* cytotoxicity of MIL-101(Cr) and H₂O₂ to mouse 4T1 breast cancer cells was also

tested as the experimental controls. Briefly, 4T1 breast cancer cells were seeded into 96-well plates ($\sim 10^4$ cells per well) and grown for 12-16 h. Then MIL-101(Cr) ($0-50 \mu\text{g mL}^{-1}$) and H_2O_2 ($0-100 \mu\text{M}$) was added to the culture. After 24h of co-cultivation, the cell viability was measured using MTT assay.

The performance of MIL-101@CoOx to mouse 4T1 breast cancer cells for an ultrasound-assisted therapy was tested. 4T1 cells were seeded in 35 mm culture dishes and incubated for 12-16 h. The medium was then replaced with fresh and serum-free culture medium containing different concentration ($0-50 \mu\text{g mL}^{-1}$) of MIL-101@CoOx or MIL-101(Cr)@CoOx + H_2O_2 ($30 \mu\text{M}$). After 4 h incubation, the cells were treated with ultrasound irradiation (1.0 MHz , 1.0 W cm^{-2}) for 3 min, and the medium was supplemented with 10% FBS. After 24h of cocultivation, the cell viability was measured by the MTT assay. CoOx with the same Co concentration as MIL-101(Cr)@CoOx was used as the experimental control.

2.7.2 Live / Dead assay

The viability of 4T1 breast cells after the ultrasound treatment was conducted using Live / Dead viability assay. Calcein-AM can be taken by live cells and converted to calcein emitting green fluorescence by intracellular esterase. PI could not penetrate the membrane of live cells, so only stain the dead cells that losing the membrane integrity. 24 h after the ultrasound treatment, the cells were stained with Calcein-AM ($4 \mu\text{mol L}^{-1}$) and PI ($8 \mu\text{mol L}^{-1}$) at 37°C for 30 min. Then the live and dead cells were observed using a fluorescence microscope (Nexcope NIB900) with excitation wavelengths of 494 nm and 535 nm, respectively.

2.7.3 Measurement of intracellular CO generation

A fluorescent probe for carbon monoxide CAY10733 was used to detect the CO production *in vitro*. Based on the Pd0-mediated Tsuji-Trost reaction, CAY10733 could release 2,7-dichlorofluorescein (DCF) in the presence of CO. The 4T1 cells were seeded in 35 mm dishes for 12-16 h, then the cells were stained with DAPI and co-cultured with MIL-101(Cr) ($34 \mu\text{g mL}^{-1}$), CoOx ($16 \mu\text{g mL}^{-1}$) and MIL-101(Cr)@CoOx ($50 \mu\text{g mL}^{-1}$). After incubation for 4 h, the cells were irradiated with ultrasound, followed with the addition of PdCl₂ and CAY10733 both with a final concentration of 1 μM . After staining at 37°C for 30 min and washing with PBS (3x), the CAY10733-labeled cells were observed using a fluorescence microscope with excitation wavelengths of 358 nm and 494 nm, respectively.

2.7.4 ROS detection *in vitro*

A fluorescent ROS probe, 2',7'-dichlorofluorescein diacetate (DCFH-DA), was used to detect intracellular ROS generation after different treatments. DCFH-DA could be taken by live cells and converted to DCF emitting green fluorescence due to the oxidation. Immediately after the sonication, DCFH-DA probe was added to the cultures, and then incubated for 30 min. The fluorescence of DCFH-DA-labeled cells was monitored using a fluorescence microscope.

2.7.5 GSH detection *in vitro*

The intracellular GSH content was examined qualitatively using a fluorescence probe naphthalene-2, 3-dicarboxaldehyde (NDA) and quantitatively using 5,5'-dithiobis-(2-nitrobenzoic

acid) (DTNB), respectively. After 2 h post ultrasound irradiation, 4T1 cells were stained with NDA (50 μM) and incubated for 30 min. The fluorescence of NDA-labeled cells was monitored using a fluorescence microscope. For quantification, 4T1 cells with different treatments were lysed with a cell lysate, and the supernatant was collected by centrifugation. DTNB was added and the absorbance was recorded by a UV-Vis spectrophotometer.

2.7.6 Mitochondrial membrane potential (MMP) assay

A fluorescent probe JC-1, which could detect the change of mitochondrial membrane potential (MMP) of cells quickly and effectively, was used to evaluate 4T1 cells after various treatments. In healthy mitochondrial with high MMP, JC-1 intends to aggregate in the matrix of mitochondrial and form J-aggregates. In damaged mitochondrial with low MMP, JC-1 could not aggregate in the matrix of mitochondrial and exist in the form of monomer. Briefly, 4 h after ultrasound treatment, the medium was replaced with 2 mL JC-1 dyeing working solution (1 \times) and the cells were incubated at 37°C for 30 min. After washing with JC-1 staining buffer (3 x). The JC-1-labeled cells were compared using a fluorescence microscope under blue and green excitation light.

2.7.7 ATP assay

To further verify the CO generation and mitochondrial dysfunction, ATP assay kit was used to assess the intracellular ATP (adenosine 5'-triphosphate) contents. The energy provided by the ATP is essential in the process of firefly luciferase and luciferin catalytic reactions. The production of fluorescence is proportional to the ATP level at a range of concentrations. In this study, 4 h after

ultrasound treatments, cell lysates were added to 4T1 breast cell culture to fully lyse the cells, the cells were then collected and centrifuged at 12000g for 5 min at 4°C. 100 µl ATP detection working solution was mixed thoroughly with 20 µl supernatant collected. The ATP contents were measured by a luminometer (Turner BioSystems, Sunnyvale, CA Patent Pending).

2.8 *In vivo* study

To further evaluate the *in vivo* antitumor properties of MIL-101(Cr)@CoOx, an 4T1 mouse tumor model developed previously^[3] was used. All animal experiments were approved by the Ethics Committee of Sir Run Shaw Hospital (ZJU20230081). 4-6 weeks old Balb/c nude mice were obtained from the Shanghai Laboratory Animal Center and were housed in a simulated cycle condition with 12 h under light and 12 h in dark cycle. After 1-week acclimatization, 50 µl PBS containing 2×10^6 4T1 cells were injected subcutaneously into the left side abdomen of nude mice to establish a tumor-bearing mouse model. Tumor-bearing Mice were randomly divided into 6 groups with different treatments as described below: (1) Control (i.v. injection of physiological saline solution); (2) US alone (1.0 MHz, 1.5 W cm⁻², 2 min); (3) MIL-101(Cr) + US (17 mg kg⁻¹, i.v. injection); (4) CoOx + US (8 mg kg⁻¹, i.v. injection); (5) MIL-101(Cr)@CoOx (25 mg kg⁻¹, i.v. injection); (6) MIL-101(Cr)@CoOx + US (25 mg kg⁻¹, i.v. injection).

The treatments were carried out at day 0, 5 and 10, and ultrasound irradiation (1.0 MHz, 1.5 W cm⁻², 2 min) were performed at 12 h and 24 h after i.v. injection of test samples. The body weight of mice and the tumor size (tumor volume = tumor length × width²/2) were closely monitored every 2 days during the whole testing period.

At the completion of the treatment period, the mice were sacrificed and the subcutaneous tumors were excised, collected, weighed and photographed. Then main organs (including heart, liver, spleen, lung and kidney) of each group were also excised and collected. The tumors and main organs were fixed with 4% paraformaldehyde solution and dehydrated, embedded in paraffin, and sectioned. Hematoxylin–eosin (H&E) or Ki-67 staining were performed in the slices.

The *in vivo* distribution of Co content in main organs (heart, liver, spleen and kidney) and tumors of mice after the injection of MIL-101(Cr)@CoOx at different time points were investigated. The collected tissue samples were weighed and digested. Then the Co contents were measured by ICP-OES.

In addition, after 1 day, 3 days and 7 days injected with MIL-101(Cr)@CoOx (25 mg kg⁻¹, i.v. injection), the blood biochemistry and hematological analysis of mice were carried out.

2.9 Statistical analysis

All data in this article are expressed as mean ± standard deviation (SD) unless otherwise noted. p-Value were determined and calculated by a student's-test. The significant difference in the data were determined when ***p < 0.001, **p < 0.01 or *p < 0.05.

Reference

- [1] Y. Ma, J. Du, Y. Fang, X. Wang, *Chemsuschem* **2021**, 14, 946.
- [2] Z. Jin, Y. Wen, L. Xiong, T. Yang, P. Zhao, L. Tan, T. Wang, Z. Qian, B.-L. Su, Q. He, *Chem. Commun.* **2017**, 53, 5557.
- [3] T. Zhang, Q. Zheng, C. Xie, G. Fan, Y. Wang, Y. Wu, Y. Fu, J. Huang, D. Q. M. Craig, X. Cai, X. Li, *ACS Appl. Mater. Interfaces* **2023**, 15, 4883.

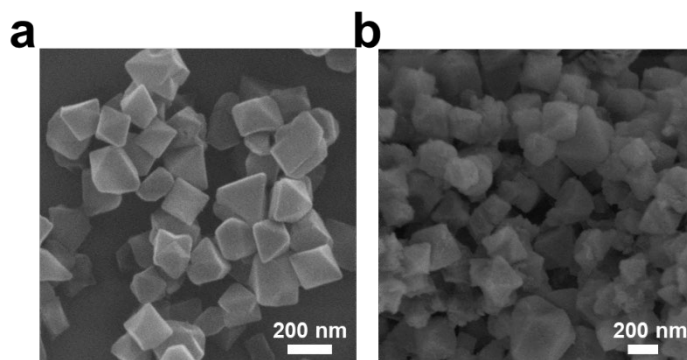


Figure S1. SEM images of (a) MIL-101(Cr) and (b) MIL-101(Cr)@CoOx.

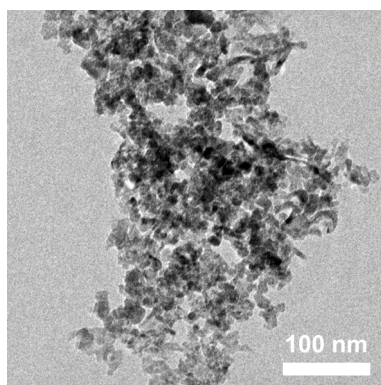


Figure S2. TEM image of CoOx nanoparticles.

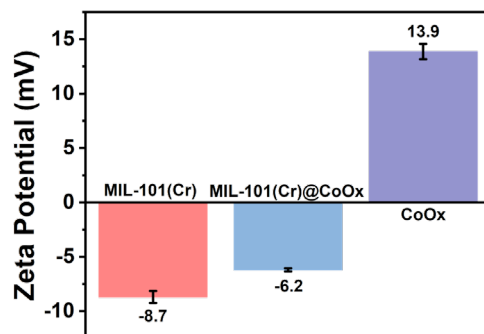


Figure S3. ζ -Potential of MIL-101(Cr), MIL-101(Cr)@CoOx and CoOx nanoparticles.

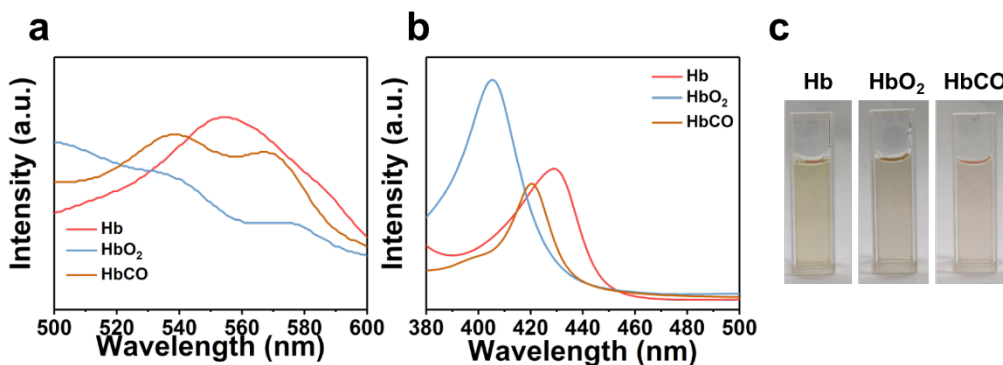


Figure S4. (a-b) UV-Vis absorption spectra of Hb, HbO₂ and HbCO. (c) The optical photographs of Hb, HbO₂ and HbCO.

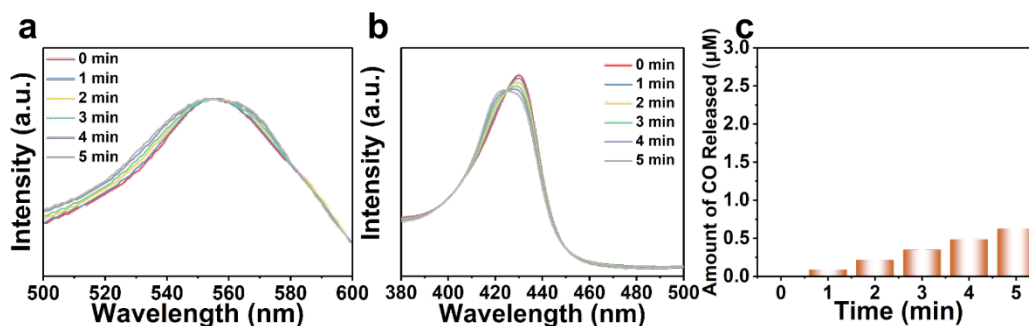


Figure S5. (a-b) UV-Vis absorption spectra of Hb (4.2 μM) with different ultrasonic vibration times (1.0 MHz, 0.5 W cm⁻²) for detecting CO generation. (c) The quantitative content of CO release under ultrasound irradiation.

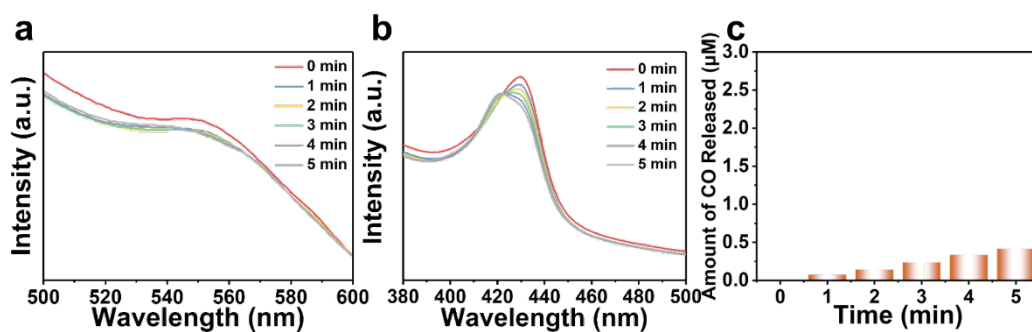


Figure S6. (a-b) UV-Vis absorption spectra of Hb (4.2 μM)/MIL-101(Cr) mixture with different ultrasonic vibration times (1.0 MHz, 0.5 W cm⁻²) for detecting CO generation. (c) The quantitative

content of CO release under ultrasound irradiation.

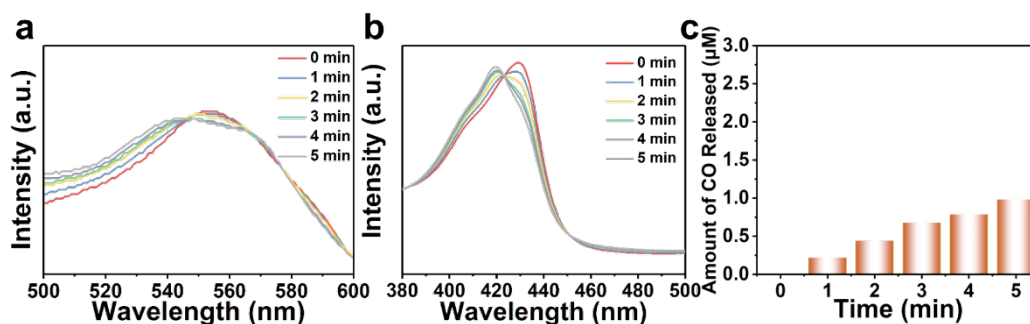


Figure S7. (a-b) UV-Vis absorption spectra of Hb (4.2 μM)/CoOx mixture with different ultrasonic vibration times (1.0 MHz, 0.5 W cm⁻²) for detecting CO generation. (c) The quantitative content of CO release under ultrasound irradiation.

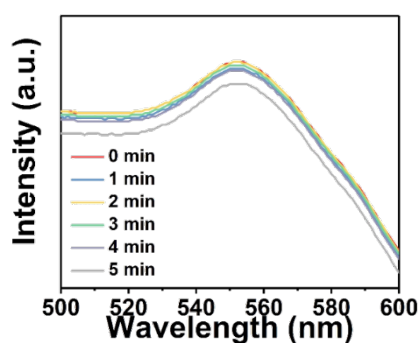


Figure S8. UV-Vis absorption spectra of Hb (4.2 μM)/MIL-101(Cr)@CoOx mixture without ultrasound treatment.

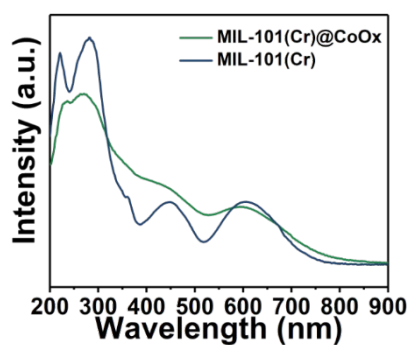


Figure S9. UV-visible diffuse reflectance spectra of MIL-101(Cr) and MIL-101(Cr)@CoOx.

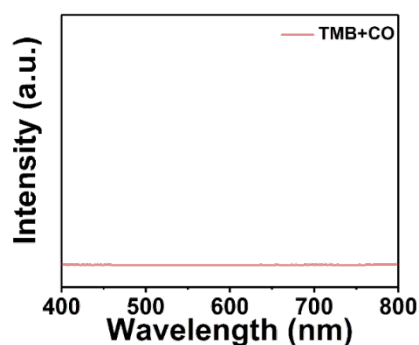


Figure S10. UV-Vis absorbance spectra of TMB solution (0.8 mM) after bubbling with CO gas.

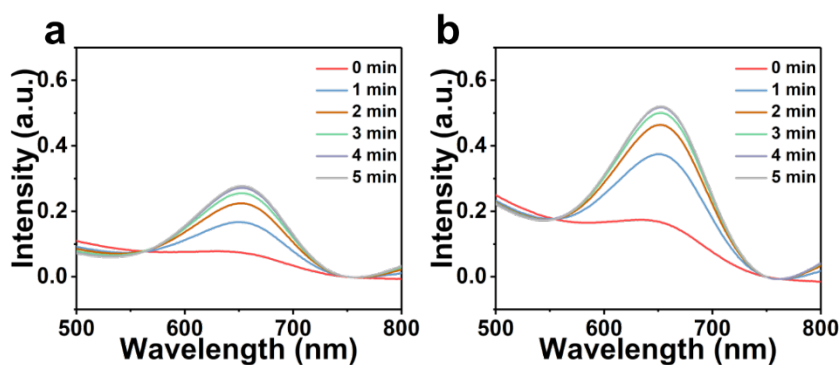


Figure S11. UV-Vis absorbance spectra of TMB solution (0.8 mM) in the presence of MIL-101(Cr)@CoO_x and H₂O₂ (a) without and (b) with ultrasound irradiation over time.

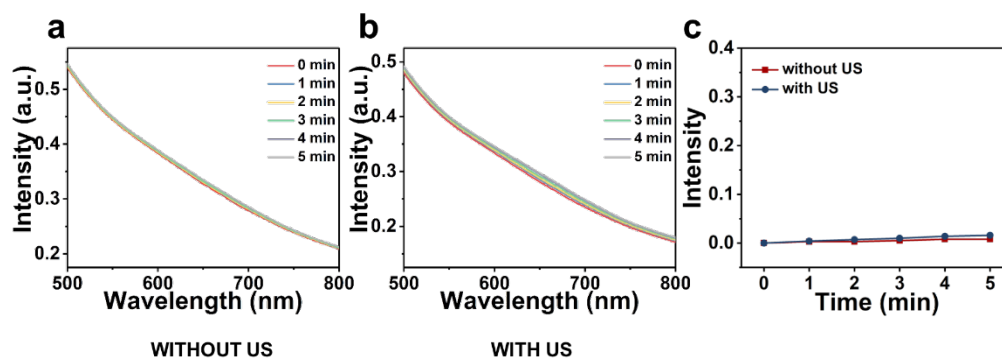


Figure S12. UV-Vis absorbance spectra of TMB solution (0.8 mM) in the presence of MIL-101(Cr) and H₂O₂ (a) without and (b) with ultrasound irradiation over time. (c) Time-dependent intensity changes at 653 nm of TMB in the presence of MIL-101(Cr) and H₂O₂ with or without US irradiation (1.0 MHz, 1.0 W cm⁻²).

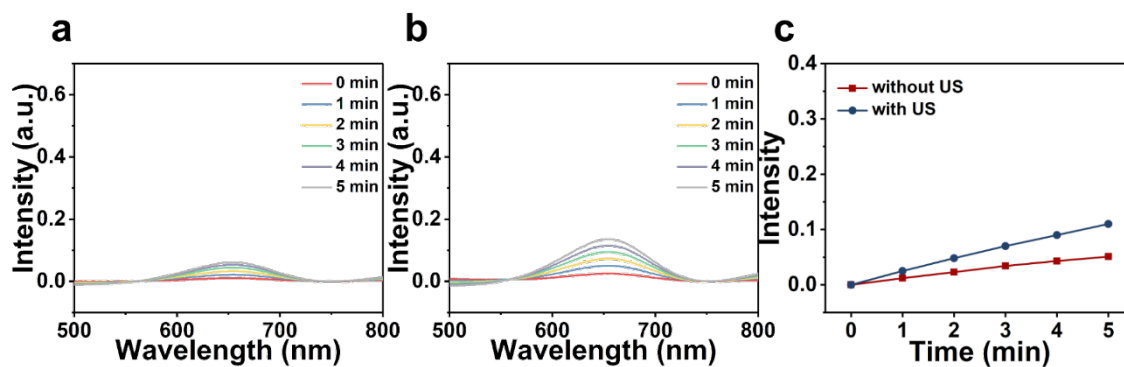


Figure S13. UV-Vis absorbance spectra of TMB solution (0.8 mM) in the presence of CoOx and H₂O₂ (a) without and (b) with ultrasound irradiation over time. (c) Time-dependent intensity changes at 653 nm of TMB in the presence of MIL-101(Cr) and H₂O₂ with or without US irradiation (1.0 MHz, 1.0 W cm⁻²).

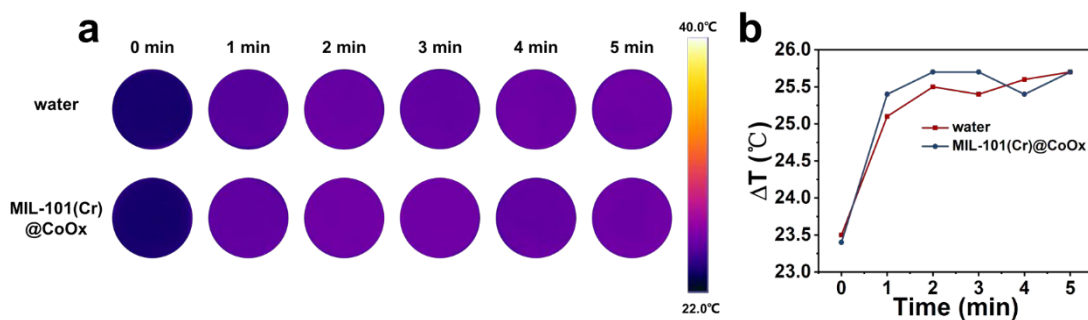


Figure S14. (a) Infrared radiation (IR) thermal images of water and MIL-101(Cr)@CoOx solution with increasing ultrasonication time. (b) The temperature change curves of water and MIL-101(Cr)@CoOx solution with ultrasound treatment.

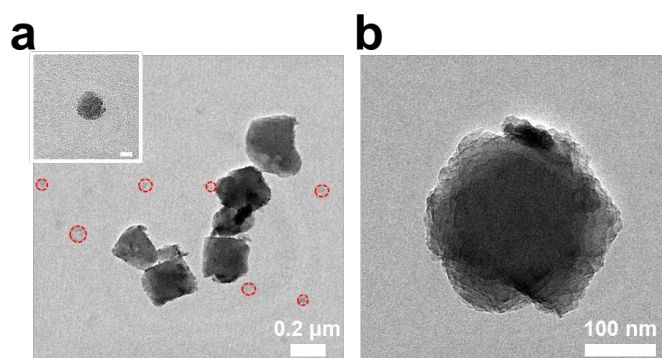


Figure S15. (a-b) TEM images of MIL-101(Cr)@CoOx nanoparticles after sonication with different

magnification (inner: a zoom-in image of the shed small nanoparticles, scale bar is 20 nm).

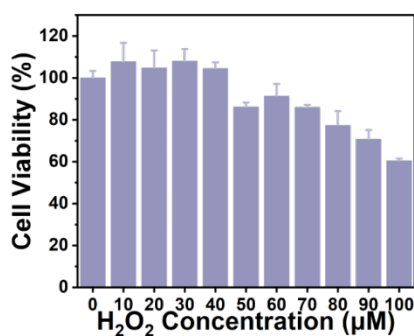


Figure S16. Cell viability of 4T1 cells incubated with H₂O₂ with different concentrations (0-100 µM).

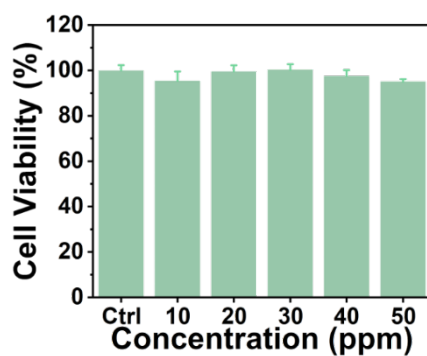


Figure S17. Cell viability of 4T1 cells incubated with MIL-101(Cr) with different concentrations.

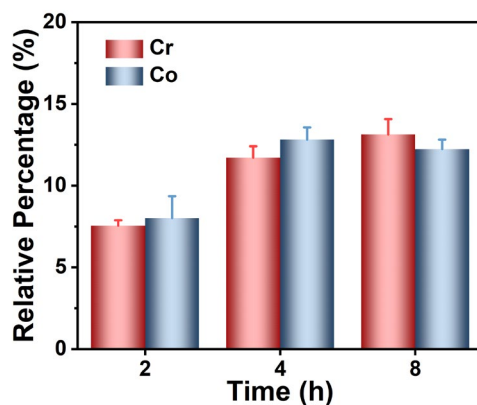


Figure S18. ICP analysis of 4T1 cells incubated with MIL-101(Cr)@CoOx for different time (n = 3, mean ± SD).

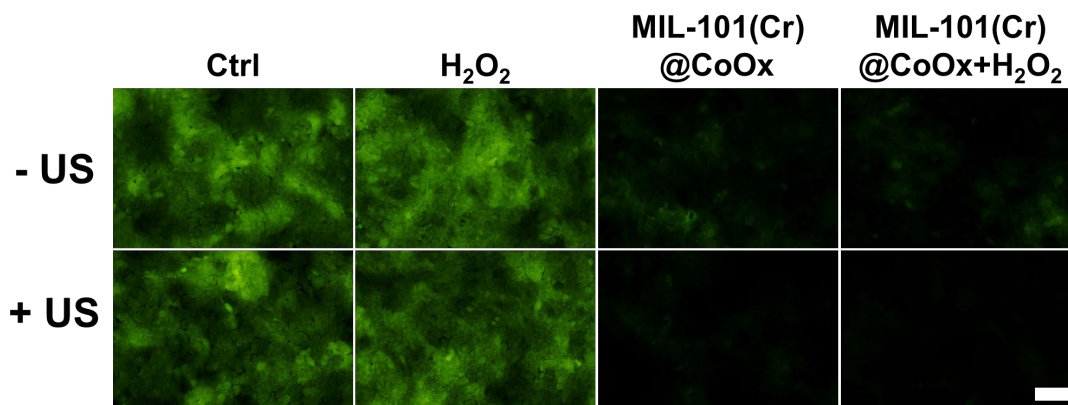


Figure S19. Intracellular GSH detection using naphthalene-2,3-dicarboxaldehyde (NDA) as a probe after incubated with different groups. Scale bar is 100 μm .

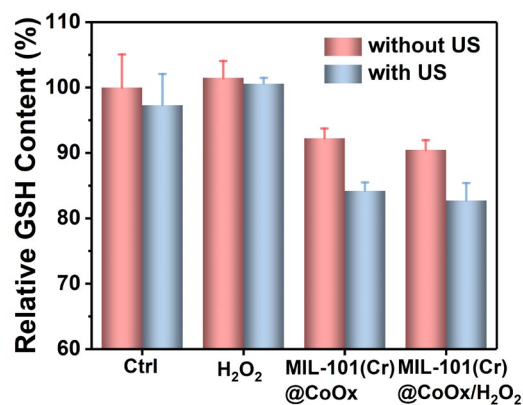


Figure S20. The GSH level of 4T1 cells after different treatments (n = 3, mean \pm SD).

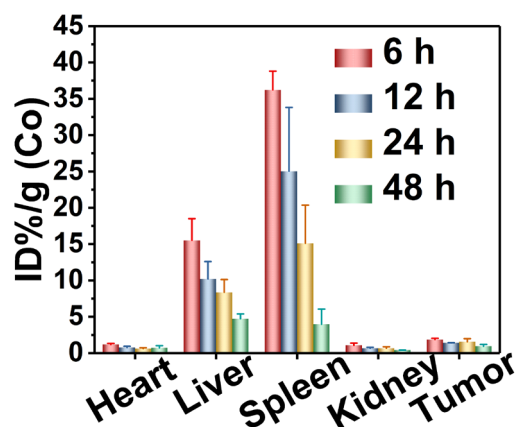


Figure S21. *In vivo* biodistribution of Co in the main organs (heart, liver, spleen and kidney) and tumor of the mice after i.v. injection of MIL-101(Cr)@CoOx for 6 h, 12 h, 24 h and 48 h (n = 3, mean

± SD).

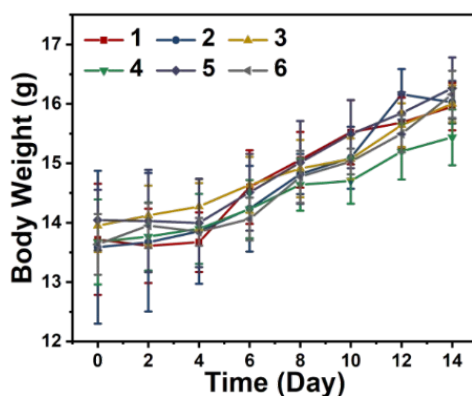


Figure S22. Body weight curve of mice after different treatments (n = 5, mean ± SD). 1: Control; 2: US; 3: MIL-101(Cr) + US; 4: CoOx +US; 5: MIL-101(Cr)@CoOx; 6: MIL-101(Cr)@CoOx +US.

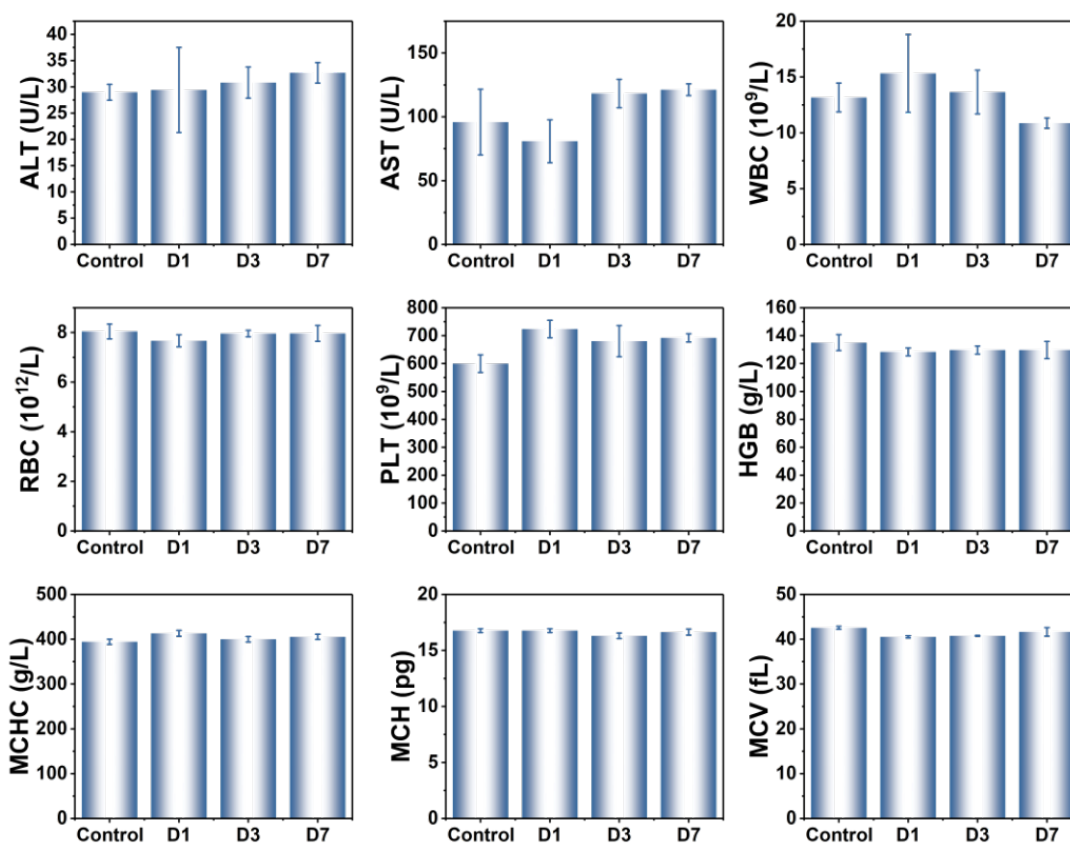


Figure S23. Blood biochemistry and hematological analysis of mice (n = 3, mean ± SD) i.v. injected

MIL-101(Cr)@CoOx with after 1 day, 3 days and 7 days, including alanine aminotransferase (ALT), aspartate aminotransferase (AST), white blood cell (WBC), red blood cell (RBC), blood platelet (PLT), hemoglobin (HGB), mean corpuscular hemoglobin concentration (MCHC), mean corpuscular hemoglobin (MCH) and mean corpuscular volume (MCV).